Journal of Materials Chemistry C

ROYAL SOCIETY OF CHEMISTRY

PAPER

Cite this: DOI: 10.1039/d4tc02096k

Non-contact computer vision enables analysis of the dynamic performance of naphthalene diimide electrochromic films†

Nicholas R. Murray,[a] Timothy J. D. McCabe,[b] Marc Reid *[b] and Emily R. Draper *[a]

Received 21st May 2024,
Accepted 5th July 2024

DOI: 10.1039/d4tc02096k

rsc.li/materials-c

Napthalene diimide-based films show effective electrochromic behaviour, with the ability to undergo a reversible transparent-to-dark colour change following the application of an electrical potential. The response of these materials is typically measured using absorption spectroscopy, however this method can be limited, especially with strongly absorbing materials. As an alternative, described herein is the application of the *Kineticolor* computer vision software platform for the camera-enabled analysis of electrochromic behaviour. Beyond monitoring of the bulk colour change of the films, studying uniformity of colour, stability, and electrochemical reversibility of film response was also undertaken. The findings illustrate an expansion of the modalities avaliable for the analysis of chromic films through a non-contact, economical and more readily deployable method than traditional spectroscopic methods.

Introduction

Electrochromic materials (ECMs) are growing in popularity in applications such as electronic displays, sensors, and smart windows.[1–5] ECMs based on organic compounds are particularly attractive due to ease of synthesis,[6] tuneability of physical and electronic properties,[7–10] and ability to be derived from renewable feedstocks.[11] In recent years, organic electrochromic (EC) films have been used in the construction of electrochromic devices (ECDs), displaying fast switching times, durability, and high colouration efficiency,[12–14] offering an alternative to traditionally used transition metal-based devices.[11] Despite this, such materials often require doping,[15] are toxic,[16] or are only processable in organic solvents.[17–19] For large-scale device construction, identifying a material that avoids these issues becomes essential.

Naphthalene diimides (NDIs) are a class of aromatic, organic small molecules known for their ability to undergo multiple reversible reduction–oxidation (redox) reactions.[20] Due to their high electron affinity and extended π-system,[21,22] NDIs can readily be reduced to form a radical anion.[11] The radical anion absorbs strongly within the visible and near infrared region of the spectrum, resulting in a strongly coloured material.[23] Conversely, NDIs in the neutral state often show the strongest absorption in the ultraviolet (UV) region of the spectrum and are therefore often colourless.[24,25] Halder *et al.* described the construction of an ECD from a sulfanilic acid-functionalised NDI film, which displayed reversible polychromic behaviour and processability in water.[26]

One of our collaborating teams has previously shown examples of NDIs in solution and as gels that show the desirable reversible colourless to dark transition.[23] It was found that the colour and performance of these materials depended on how they aggregate in solution, which was directly related to the apparent pK_a of the different NDIs.[27,28] However, liquid based ECDs can have problems with leakage, stability and in their preparation.[23,27,29,30] It has been shown that development of film-based ECDs mitigates leakage, and makes them more easily scalable.[31,32] Films made from small molecules often do not have sufficiently robust mechanical properties and so are often brittle and prone to cracking, resulting in device failure.[33] Therefore it is often necessary to employ a polymer additive in the construction of films to add in the required mechanical properties. Hyaluronic acid (HA) is a naturally occurring polysaccharide that has been previously used in the formation of polymeric films.[34–36] HA is an ideal polymer for our purposes due to its high degree of water solubility,[35] allowing for films to be fully processable in water. This avoids the use of synthetic polymers, which pose a greater environmental risk.[37] The resulting NDI/HA film can then be utilised as an ECD.

[a] School of Chemistry, JBB University of Glasgow, G12 8QQ, UK. E-mail: Emily.Draper@glasgow.ac.uk
[b] Department of Pure & Applied Chemistry, University of Strathclyde, Royal College Building 204 George Street, Glasgow, G1 1XW, UK. E-mail: marc.reid.100@strath.ac.uk

† Electronic supplementary information (ESI) available. See DOI: https://doi.org/10.1039/d4tc02096k

For this work, we prepared amino-acid functionalised NDIs with HA films and assessed their suitability for use in ECDs. The response of NDIs in solution is typically measured using absorption spectroscopy,[27] however this approach presents several challenges when measuring a material that is very strongly absorbing or concentrated into a film for example. Therefore, measurements on films are typically moved between an electrochemical set-up into a spectrophotometer, or by use of a spectroelectrochemical (SEC) cell.[26,38] The use of a SEC cell can often not be representative of an ECD, due to the size and electrodes used. When using separate pieces of equipment, this results in longer experiment times while increasing the risk of film damage. For our NDI films, the reduced sample can oxidise in air, resulting in a non-representative measurement. Also due to the strong absorbance displayed by the reduced NDI,[27] it is likely that the coloured film will fall out with the range measurable by the spectrometer. Measurements of >1.0 are considered unreliable for many spectrometers.[39] This also does not tell you what amount of reduction is needed for the film to visibly stop changing colour (by eye), only about the amount of radical present. A solution to this analytical problem involves sample dilution, however reducing the concentration of the NDI could interfere with the EC behaviour of the film and would therefore not be representative of the EC device. Reflectance spectroscopy can be used to measure untransparent solid-state samples and is therefore a popular technique in monitoring the response of EC films,[40–42] avoiding the need for sample dilution. Although the information gained from spectroscopy is vital in our understanding of EC materials, these methods cannot be easily used to measure the uniformity of the colour change or quantify specific colour variations as seen by eye. Furthermore, due to the expense of spectrophotometers, such analysis may not be readily available to researchers. Therefore, identifying an alternative method of measuring the behaviour of the film that can be used in conjunction with the aforementioned techniques is critical to the development and use of ECDs.

As a candidate alternative approach to analysing electrochromic materials, one of our teams has developed the computer vision software *Kineticolor* enabling colour-derived kinetic analysis from video footage, with existing applications including catalyst activity,[43] mixing analysis,[44] forensic drug testing,[45] and peptide synthesis.[46] This is achieved by recording the reaction of interest with any camera and using the resulting video as input for *Kineticolor*. It can calculate the colour composition of reaction bulk over time (*i.e.*, in RBG, HSV, and L*a*b* colour models), as well as quantities like contrast change (ΔE, derived from Euclidean distance in the L*a*b* colour space). From these non-contact data, the kinetics of the bulk reaction progress can be inferred.[44] While optical parameters like ΔE can be generated from traditional reflectance spectra or by using other commercial systems, *Kineticolor* integrates optical analysis with both time and spatially resolved metrics in a single platform. Furthermore, due to the accessibility and portability of digital cameras, computer vision analysis can easily be used with different experimental set-ups and

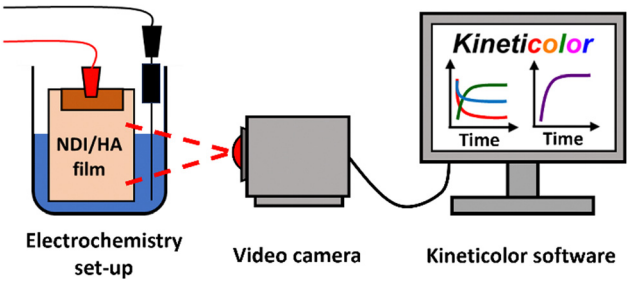

Fig. 1 Cartoon showing the use of non-contact computer vison analysis as a means of monitoring the EC behaviour of NDI-based films.

in resource-limited research settings,[47] providing a time and cost-effective way of monitoring chemical processes that complements traditionally used spectroscopic methods. The software can be used for any system that changes colour but has not been utilised in the study of EC reactions before the present study.

Here, we report the use of *Kineticolor* as a means of providing time- and spatially-resolved non-contact monitoring the EC behaviour of NDI-based films. This approach is represented graphically in Fig. 1. Although this method provides additional analysis at the expense of detailed spectral information, when used in conjunction with traditional spectroscopic techniques we aim to gain a more robust understanding of the EC response of our materials. Electrochemical reduction and oxidation have been performed on the NDI films, the resulting colour changes from which have been video recorded and analysed with *Kineticolor*.

Results and discussion

For this study, NDIs appended with the amino acids L-leucine (**NDI-L**) and L-methionine (**NDI-M**) were used (Fig. 2). Both materials are known to undergo colour changes upon electrochemical reduction. **NDI-L** undergoes a colourless to dark (apparent black) change, and **NDI-M** a yellow to orange transition. These NDIs were chosen to assess the suitability of computer vision analysis for monitoring these types of electrically-triggered solid state colour changes. Their

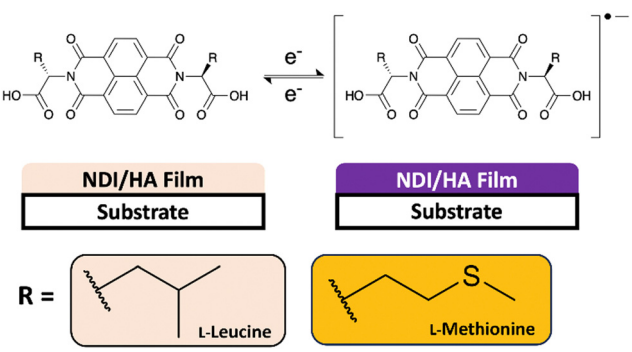

Fig. 2 Cartoon showing an NDI/HA film in the colourless neutral state (left) and the coloured reduced state (right). "R" represents the amino acid side chain of **NDI-L** (L-leucine) or **NDI-M** (L-methionine).

colouration efficiencies are provided in Table S1, and Fig. S10, ESI.†

From previous studies, one of our teams has shown that the pH and concentration of the NDI in solution influences their behaviour and so **NDI-L** was prepared at pH 9 and **NDI-M** at pH 6 at a concentration of 5 mg mL^{-1}. At these pHs in solution, the compounds showed their strongest colour change (Fig. S13–S20, ESI†).[23,27]

To measure the EC response of the films a three-electrode set-up was used, with a supporting electrolyte of 0.1 M tetrabutylammonium hexafluorophosphate (TBAHFP) in dichloromethane (DCM). FTO and platinum wire served as the working and counter electrode, respectively. An organic reference electrode containing 0.01 M silver nitrate ($AgNO_3$) in acetonitrile was used. The films were electrochemically reduced by applying a potential of −1.8 V. This potential was determined from cyclic voltammetry (CV) measurements (Fig. S22, ESI†). Both films underwent a change in their absorbance, with several new peaks appearing within the visible region indicative of the radical anion (Fig. 3a and b).[27] **NDI-L** changes from a colourless neutral state to a dark purple reduced state (Fig. 3c), while **NDI-M** underwent a yellow-to-orange transition (Fig. 4d). Upon oxidation, both the **NDI-L** and **NDI-M** films showed a partial or total restoration of original colour due to the reformation of the neutral species (Fig. S23 and S24, ESI†). The **NDI-L** film showed stronger absorbance following reduction, likely meaning that more of the reduced species was being formed. This suggests, as with NDIs in solution, that the choice of amino acid can have a drastic effect of the EC properties of the compound (Fig. 3c and d).[27] After 20 minutes of reduction, several of the **NDI-L** peaks fall out-with the range that is considered measurable.

To make best use of the computer vision analysis, untested NDI films were reduced with the electrochemical set-up placed in a lightbox with the camera, minimising any influence of ambient light on the video footage collected for analysis. This set-up serves to standardise and control lighting conditions,

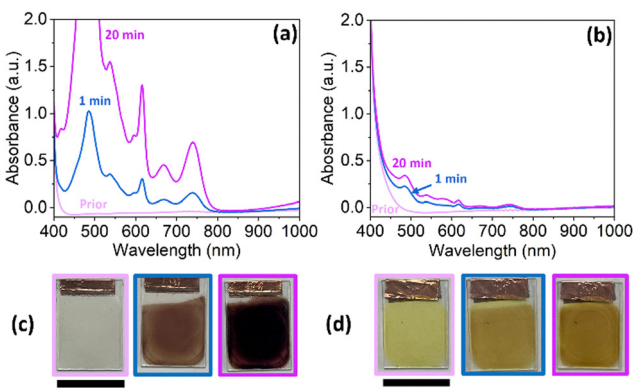

Fig. 3 Absorbance of (a) **NDI-L** and (b) **NDI-M** films prior (—) to application of potential and after application of −1.8 V for 1 minute (—) and 20 minutes (—). Inset images of the (c) **NDI-L** and (d) **NDI-M** films prior to reduction (left) and after application of −1.8 V for 1 minute (middle) and 20 minutes (right). Scale bar is 15 mm.

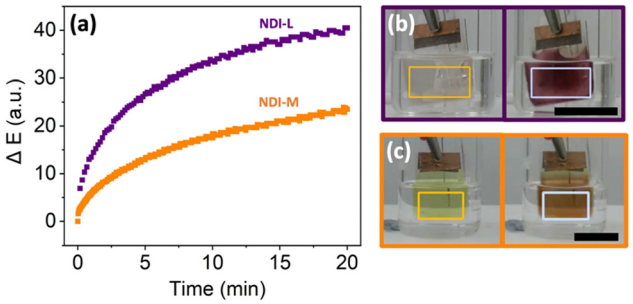

Fig. 4 ΔE of **NDI-L** (■) and **NDI-M** (■) film over time upon the application of −1.8 V. Images of **NDI-L** film (b) and **NDI-M** film (c) prior to reduction (left) and following application (right) of −1.8 V for 20 minutes. Scale bar given is for 15 mm. Square outline on images represents area processed by *Kineticolor*.

analogous to conventional spectroscopic methods. As shown in Fig. 4a, both NDI films resulted in a measurable increase in ΔE (colour-agnostic contrast change since time zero) over the duration of the electrochemical experiment. This quantitative and time-resolved observation is consistent with what we see and describe qualitatively by eye, and by UV-vis absorption spectroscopy, that a large change in colour has occurred. Of the two NDI films, the **NDI-L** film recorded a greater ΔE over the chosen experiment time due to the formation of a larger amount of the radical anion, as confirmed by absorption measurements. This highlights that, by using *Kineticolor* in conjunction with spectroscopy, we were able to gain a more comprehensive understanding of the EC behaviour of the NDI materials of interest. Upon the application of an oxidising potential, the **NDI-L** film showed partial restoration of its initial colour, whilst the **NDI-M** film appeared irreversible (Fig. S25, ESI†). We hypothesised that both the photo- and electrochemical sensitivity of the NDI films could be playing a role in attenuating the oxidation of the films. As a control, experiments were performed to assess the photosensitivity of the NDI films in the absence of electrical stimulus. It was found that **NDI-M** exhibited higher sensitivity to the lighting conditions used than **NDI-L**, and although this did not contribute significantly to the colour change on the timescale of the electrochemically-induced colour changes, it did however mean that the oxidation back to the initial state proved more difficult than anticipated (Fig. S26 and S27, ESI†). The EC response of the **NDI-L** film was also monitored outside of the lightbox to investigate the influence of uncontrolled lighting on the *Kineticolor* output (Fig. S28, ESI†). The ΔE values followed a similar trend over time to that collected inside the lightbox, albeit with an overall weaker response. However, this served to highlight that meaningful insights can still be gained in instances where controlled lighting is not possible. *Kineticolor* was also used to monitor the electrochromic response of other systems. Perylene bisimide (PBI) based films were prepared and electrochemically reduced. As with NDIs, this results in the formation of a radical anion, and a change in colour of the material.[48] This change is quantified by a measurable increase in ΔE over time (Fig. S29, ESI†), thereby

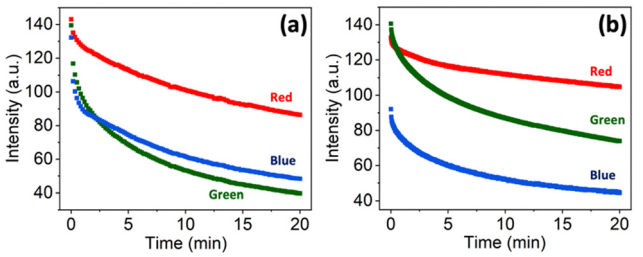

Fig. 5 RBG plot showing intensity of red (■), green (■), and blue (■) colour components of **NDI-L** film (a) and **NDI-M** film (b) upon application of −1.8 V for 20 minutes.

confirming that computer vision analysis can readily be utilised in the study of other ECDs.[49]

Beyond ΔE trends, additional outputs are generated by *Kineticolor* to help quantify colour intensity and specific colour change variations. These outputs include the RGB time series, showing the variation in the proportion of the red, green, and blue colour components over time. These values are critical in the context of applications such as smart glass and windows. Although RBG values can be generated from absorption data, this requires additional processing and may be unreliable with strongly absorbing materials such as our NDI films. RGB graphs were created for both films (Fig. 5). Prior to reduction, the **NDI-L** film showed a similar intensity for all colour components, resulting in a near colourless film with low colour saturation. The **NDI-M** films showed a lower intensity of blue, indicating a yellow-coloured film. Upon reduction, both films showed a decrease in the intensity of red, green, and blue, resulting in a darkening of both films, however the extent by which the colour channel intensities changed varied between NDI films. The relative intensities of the green channel for each NDI film were notably different following reduction, resulting in the colour difference observed between the reduced films. Additional outputs such as HSV (hue, saturation, and value) and L*a*b* (lightness and a/b components) were created as an alternative representation of this colour change (Fig. S30 and S31, ESI†). Upon oxidation, the **NDI-L** film showed an increase of all three RGB colour components, resulting in a lightening of the NDI film caused by the reformation of the neutral species (Fig. S32, ESI†). For **NDI-M**, the RGB values did not change in response to oxidative conditions, meaning the initial colour (before reduction) was not restored, consistent with the spectroscopic results (Fig. S33, ESI†).

We next investigated the colorimetric aspects of the electrochemical reduction on the **NDI-L** film in more detail with *Kineticolor*. As shown in Fig. 6a, the film appeared to undergo most of the overall colour change within the first 20 minutes of the electrochemical reaction. Beyond this point, there was no significant change in ΔE, despite absorption measurements showing an increase in the concentration of radical present (Fig. 6b). This showed that the NDI film had reached its peak colour saturation by this stage of the reaction, and any longer reduction was increasing the radical concentration, not the visible colour that is important for downstream applications of

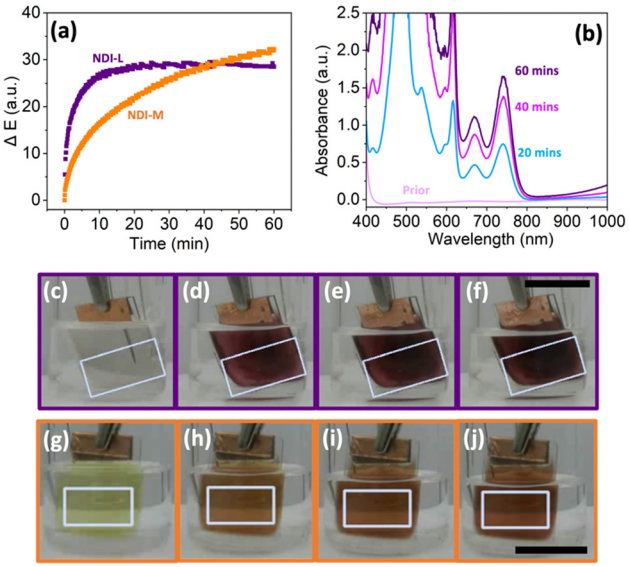

Fig. 6 (a) ΔE trends over time for **NDI-L** (■) and **NDI-M** (■) films upon application of −1.8 V for 60 minutes. 0 minutes marks the pointed of electricity being applied. (b) Absorbance data of **NDI-L** film prior (—) to application of potential and after application of −1.8 V for 20 minutes (—), 40 minutes (—), and 60 minutes (—). Insert images of **NDI-L** (top row) **NDI-M** (bottom row) films prior to (c) and (g) application of potential and after application of −1.8 V for 20 minutes (d) and (h), 40 minutes (e) and (i), and 60 minutes (f) and (j). Scale bar is for 15 mm. White square outline on each image (c)–(j) represents area processed by *Kineticolor*.

these films. Indeed, the camera-enabled measurements presented a means by which to understand when to stop reduction at the earliest point and mitigate the risk of making the oxidation more difficult from generating surplus radical anion. This is reflected in images taken of the films, which show negligible increase of colour after 20 minutes (Fig. 6b–e). This equilibrium point is also plotted using the alternative colour metrics – RGB, HSV and L*a*b* – to provide alternative visualisations of the same phenomenon (Fig. S34, ESI†). This experiment was repeated with **NDI-M**, however, the ΔE increased consistently for the duration of the experiment (Fig. 6a). Images taken show that the film continues to darken by eye during this time (Fig. 6g–j). This could suggest that the coloration process is less efficient than for **NDI-L**, thereby requiring longer reduction times to reach maximum colour saturation. Alternatively, due to the light sensitivity displayed by the **NDI-M** film, the film may be continuously reducing due to the influence of the LED lights.

The homogeneity of the colouration process was also investigated. Rather than observing only the globally averaged colour change undergone by a reaction, *Kineticolor* can break down the measured area into smaller components, from which spatially-resolved kinetics outputs can be generated.[44] This approach enabled comparison of ΔE trends at different sections of the NDI film, for example the edge *versus* the middle of the film. This spatial disparity is an important consideration for real-world ECDs, where a uniform EC response is required. As a spectrophotometer can only measure a single point of a sample

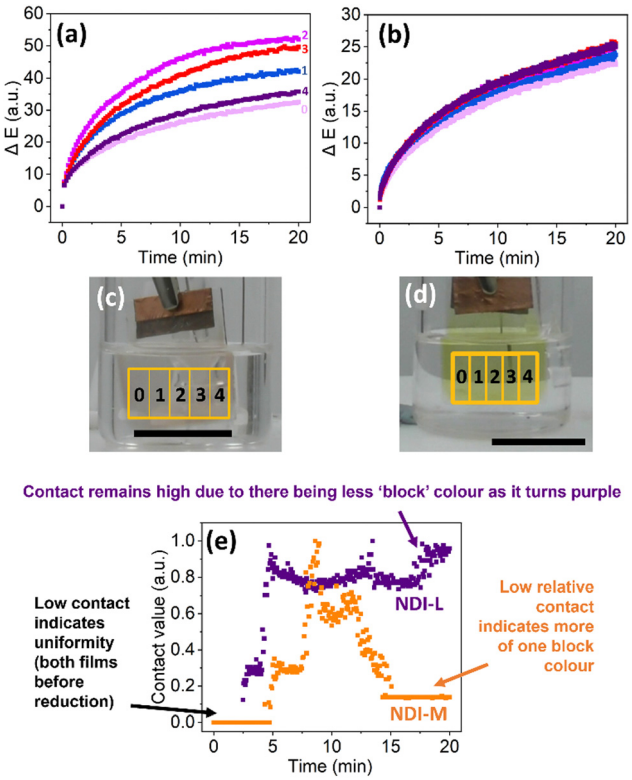

Fig. 7 Area specific response of **NDI-L** (a) and **NDI-M** (b) films upon application of −1.8 V for 20 minutes, showing ΔE of column 0 (■), 1 (■), 2 (■), 3 (■) and 4 (■). Image of **NDI-L** (c) and **NDI-M** (d) films prior to reduction, showing the position of corresponding columns. (e) Annotated contact analysis of **NDI-L** (■) and **NDI-M** (■) films upon application of −1.8 V for 20 minutes. Scale bar is for 15 mm.

at once, it is difficult to measure the real-time uniformity *via* conventional absorption or reflectance measurements. While other techniques like imaging spectroscopy and hyperspectral imaging can provide spatial information,[43] such methods often require more expensive or complex equipment. Computer vision analysis therefore provides a more accessible and cost-effective means of obtaining spatial information. As shown in Fig. 7, the measured area of the **NDI-L** film from the video recording was separated into several columns and the ΔE was calculated for each. Upon reduction, there is variation in ΔE across the film. The strongest change was observed in columns 1, 2, and 3, which corresponded to the centre of the film. The weakest change was observed in columns 0 and 4, corresponding to the edges of the film. This spatial analysis showed that the most pronounced colour change and thus EC response was occurring at the centre of the film, likely because of non-uniform distribution of the NDI across the substrate. This inhomogeneity likely arose during the thermal annealing stage of film preparation where, upon evaporation of the solvent, the NDI became more concentrated at the film's centre. A similar phenomenon has been observed in the preparation of other films.[50] By comparison, the **NDI-M** film underwent a more uniform change in colour, suggesting an even distribution of the NDI across the substrate. Assuming no mechanical fault in the film fabrication, the root cause of the different uniformity of NDI distribution could be the result of the different amino acid groups affecting the hydrophobicity of the solution and therefore affecting the drying on the glass substrate. For example, it has been shown that changing the amino acid group can alter the viscosity and hydrophobicity of NDI and other rylene-based solutions.[27,51] The methionine group in **NDI-M** is more soluble in water than leucine in **NDI-L** and therefore may wet the surface of the glass substrate more effectively, and thus be less susceptible to drying effects. A similar experiment was performed using UV-vis absorption spectroscopy, where different areas were measured to assess homogeneity of the film (Fig. S35, ESI†). These were difficult to carry out, as the films were moved between the electrochemical set up and the spectrophotometer. This allowed oxidation to occur and damage of the films with handling. We were unable to accurately choose points to analyse. This is where again *Kineticolor* has the advantage, as we did not need to move the films and could choose to look at any part of the film using the software. We could then go back to the same image and analyse another part of the film, without having to remeasure. Texture-derived analysis was generated from this video footage to further investigate the heterogeneity of the coloration over time. Contact analysis was performed on both films. Using *Kineticolor*, each video frame was converted into a binary image, and each pixel within the region of interest was coloured either white or black, depending on whether they were darker than a user selected grayscale threshold.[44] By calculating the perimeter between the white and black pixels, contact values were generated. As the user can set the greyscale threshold, contact can be used to quantify small but distinct spatial effects. As shown in Fig. 7e, while the **NDI-M** film shows a local minimum towards the end of the reduction, indicating homogenous colouration, the **NDI-L** values increase over time and remain high for the duration of the experiment, demonstrating a less uniform colour change. These results corroborate the observed ΔE trends. Additional texture derived analysis was performed, showing the contrast, homogeneity, energy, and entropy of these materials upon reduction (Fig. S36–S39, ESI†). The results gained from these measurements further support the previously described observations of film homogeneity and highlights the large amount of spatial and time-resolved data that can be generated from a single video using *Kineticolor*.

When considering the applicability of such materials in real-world device construction, it is important that the NDI film shows consistent EC behaviour over multiple redox cycles. Devices based on organic materials have previously been shown to display electrochromic stability across thousands of cycles.[52,53] The cyclability of films is typically investigated using spectroscopy, but this analytical method presents several challenges, including long experiment times and risk of film damage from moving the film between spectrophotometers and the EC set up. Instead, we applied computer vision analysis to monitor the cyclability of the **NDI-L** film in an in-line, non-contact fashion, requiring no transfer of the materials of interest in and out of the reactive environment. A reducing

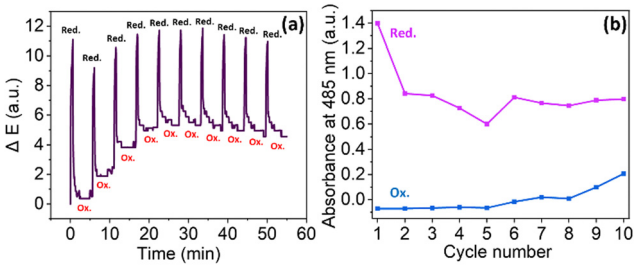

Fig. 8 (a) ΔE of **NDI-L** film throughout 10 redox cycles. Films were reduced *via* application of −1.8 V for 30 seconds and oxidised *via* application of 1.6 V for 5 minutes. (b) Absorbance at 485 nm of **NDI-L** film throughout 10 redox cycles. Films were reduced *via* application of −1.8 V for 30 seconds and oxidised *via* application of 2.0 V for 5 minutes. "Red" and "Ox" represents when the film is in the reduced and oxidised state, respectively.

potential was applied for 30 seconds, followed by an oxidising potential for 5 minutes. As shown in Fig. 8, the ΔE of the oxidised state increases over the first few cycles before plateauing. This oscillation pattern suggests that the oxidation is becoming less efficient over time. This phenomenon has been observed for NDIs in solution, where the resistivity of the material increases upon cycling, thereby making oxidation progressively slower.[27] Following a drop after the first cycle, the ΔE of the film in the reduced state remained stable for the duration of the experiment, relating to a consistent change in colour seen by eye with each reduction. Similar behaviour is observed using absorption spectroscopy, again showing how NDI EC behaviour is linked to the presence of the radical anion (Fig. 8b). This data suggest that the **NDI-L** based films show cyclability across the first ten cycles, upon which the experiment was halted due to evaporation of the DCM. It should be noted that the ΔE of the recorded film does not entirely correspond to the absorption measurements. For example, the absorbance in the reduced state does not return to its initial value and the absorbance of the oxidised state grows steadily after several cycles. These disparities could result from differences in the experimental set-up (*i.e.* different oxidising potentials and lighting conditions). Alternatively, if the film coloration becomes less homogeneous upon cycling, this would not be reflected in the absorbance data, resulting in a non-representative result. As computer vision analysis can measure the entirety of the film, this provides a more accurate representation of cyclability and could explain the differences observed between ΔE and absorbance. The performance of **NDI-M** was also measured under these conditions. These films showed less reversibility we think due to the **NDI-M** being more light sensitive (Fig. S40, ESI†).

Conclusions

In summary, non-contact and camera-enabled computer vision analysis has presented a powerful in-line alternative approach to spectroscopic methods and has enabled data-rich monitoring of EC behaviour of films in their representative device-specific environment. With only a video camera required, this analytical approach is easily utilised in different research environments and is not limited by scale. For NDI film analysis, the need for a spectrophotometer was circumvented. While absorption measurements quickly fall out of measurable range, computer vision analysis (demonstrated here with *Kineticolor*) accurately tracked the changes undergone by the films for the duration of an experiment, and throughout several redox cycles. We also investigated specific colour change variations, colouration homogeneity, and colour saturation times, information which would be crucial in the development of ECDs and would be unattainable when relying solely on other, more invasive analytical techniques. We envisage that the computer vision approach exemplified in this study will simplify the non-destructive characterisation and design of more stimuli-responsive materials.

Experimental

Full experimental methods and protocols are provided in Section S1 of the ESI.† Further details on spectroelectrochemisty, cyclic voltammetry, UV-vis absorption spectroscopy, control studies, and *Kineticolor* outputs can be found in Section S2 of the ESI.†

Synthetic procedures

The NDIs were synthesised *via* a reaction between naphthalene-1,4,5,8-tetracarboxylic acid dianhydride and an amino acid in the presence of molten imidazole. This was performed following standard protocols.[27] The full synthetic procedure and characterisation is provided in the ESI† in Section S1.

Film formation

Solutions were prepared at a concentration of 5 mg mL^{-1} of NDI. The solid NDI was dissolved in 2 molar equivalents of NaOH (aq, 1 M). The remainder of the solution was made up with deionised water. HA was added at a concentration of 15 mg mL^{-1}. This polymer concentration was chosen as it produced a very viscous solution that dried into suitably uniform and unbroken films. Prior to casting, the solutions were adjusted to pH 9 and pH 6 for NDI-L and NDI-M respectively. Solutions were cast using a doctor blade onto FTO glass at a thickness of 1.5 mm, and thermally annealed at 80 °C for 60 minutes. The glass was cleaned using oxygen plasma for 20 minutes for a more hydrophilic surface on which the films can adhere to. The glass was used immediately after plasma cleaning.

Electrochemistry

Electrochemical reduction and oxidation were performed using a PalmSens4 potentiostat. A three-electrode setup was utilised for all measurements. To test the films, an electrolytic solution of DCM and TBAHFP was prepared and degassed with nitrogen gas for 10 minutes. The film coated FTO glass, functioning as a working electrode, was suspended in the solution, in addition

to a platinum wire counter electrode and an organic reference electrode containing 0.01 M $AgNO_3$ in acetonitrile. Both **NDI-L** and **NDI-M** films were reduced using a potential of −1.8 V. This voltage was chosen from CV measurements. To oxidise the film, a large oxidising potential was required. For absorption measurements, a voltage of 2.0 V was used to oxidise the film. For *Kineticolor* measurements a voltage of +1.6 V was used; using the lower voltage ensured that the solvent was not electrochemically affected which would interfere with the video measurement and resulting *Kineticolor* output.

UV-vis absorption spectroscopy

The absorbance of the film was measured using a Cary 60 UV-visible spectrophotometer from Agilent technologies. Spectra were collected from 300 nm to 1000 nm, and a scan rate of 600 nm min^{-1} was used. Baseline measurements were performed on clean FTO glass. A 3D-printed holder was used for all film measurements. This ensured the area measured by the spectrometer remained consistent. The films were measured before and immediately after the desired electrochemistry was performed. Photographs were taken of films after each measurement.

Computer vision analysis with *Kineticolor*

The EC response of the film was monitored using a Panasonic HC-W580, filming at a resolution of 780p and 25 frames per second. All videos were recorded with manual focus and no auto white balance. These settings avoided any changes in focus or video quality for the duration of each experiment. All electrochemical measurements recorded on video were performed in a light box to minimise the effects of ambient light. The camera was also placed inside the lightbox, thereby allowing filming to be undertaken within a completely enclosed lightbox. The two LED light panels were kept on at full power for the duration of each experiment. This ensured the set-up was well lit and the video output was of good quality. The resulting video files were uploaded to and processed using *Kineticolor*. The analytical workflow has also been described elsewhere.[44,45] Outputs included colour and mixing time series. Still images of NDI films included in the manuscript were taken from video recordings. For contact analysis a greyscale threshold of 80 was used for both films.

Author contributions

Conceptualisation – MR, ED; methodology – NM, TM, MR, ED; validation – NM, TM; formal analysis – NM, TM; investigation – NM, TM, MR, ED; data curation – NM; writing – all; review and editing – all; visualisation – NM; supervision – MR, ED; project administration – ED; funding acquisition – MR, ED.

Data availability

All data in this document is displayed in the ESI.† This includes all characterization and preparation methods. If the data has been processed this has been described in the paper or ESI.† Images have not been altered in any way and are used as collected. For raw data collected, this available upon request from the authors.

Conflicts of interest

M. R. is the inventor of *Kineticolor* and is leading the disclosure of the technology for commercialisation. Please refer to co-corresponding author details for details on obtaining a *Kineticolor* software license.

Acknowledgements

N. R. M. thanks the EPSRC (EP/T517896/1) for funding. E.R.D thanks the UK Research & Innovation for Future Leaders Fellowship funding (MR/V021087/1). These authors also thank Dr Alan Wiles for construction of doctor blade, and Professor Peter J. Skabara for use of plasma cleaner. T. J. D. M. and M. R. thank the UK Research & Innovation for Future Leaders Fellowship funding (MR/T043458/1).

Notes and references

1 C. Gu, A.-B. Jia, Y.-M. Zhang and S. X.-A. Zhang, *Chem. Rev.*, 2022, **122**, 14679–14721.
2 G. Mehlana and S. A. Bourne, *CrystEngComm*, 2017, **19**, 4238–4259.
3 C. M. Lampert, *Mater. Today*, 2004, **7**, 28–35.
4 B. F. Urbano, S. Bustamante, D. A. Palacio, M. Vera and B. L. Rivas, *Polym. Int.*, 2021, **70**, 1202–1208.
5 J.-L. Wang, S.-Z. Sheng, Z. He, R. Wang, Z. Pan, H.-Y. Zhao, J.-W. Liu and S.-H. Yu, *Nano Lett.*, 2021, **21**, 9976–9982.
6 R. J. Mortimer, *Electrochim. Acta*, 1999, **44**, 2971–2981.
7 T. A. Welsh, O. Matsarskaia, R. Schweins and E. R. Draper, *New J. Chem.*, 2021, **45**, 14005–14013.
8 M. Olesińska, G. Wu, S. Gómez-Coca, D. Antón-García, I. Szabó, E. Rosta and O. A. Scherman, *Chem. Sci.*, 2019, **10**, 8806–8811.
9 F. S. Etheridge, R. Fernando, J. A. Golen, A. L. Rheingold and G. Sauve, *RSC Adv.*, 2015, **5**, 46534–46539.
10 J. Shukla and P. Mukhopadhyay, *Eur. J. Org. Chem.*, 2019, 7770–7786.
11 T. A. Welsh and E. R. Draper, *RSC Adv.*, 2021, **11**, 5245–5264.
12 C. Park, J. M. Kim, Y. Kim, S. Bae, M. Do, S. Im, S. Yoo and J. H. Kim, *ACS Appl. Electron. Mater.*, 2021, **3**, 4781–4792.
13 C. Gu, S. Wang, J. He, Y.-M. Zhang and S. X.-A. Zhang, *Chem.*, 2023, **9**, 2841–2854.
14 A. Chaudhary, D. K. Pathak, M. Tanwar, P. Yogi, P. R. Sagdeo and R. Kumar, *ACS Appl. Electron. Mater.*, 2019, **1**, 58–63.
15 T.-R. Chou, S.-H. Chen, Y.-T. Chiang, T.-T. Chang, C.-W. Lin and C.-Y. Chao, *Org. Electron.*, 2017, **48**, 223–229.
16 V. Annibaldi and C. B. Breslin, *J. Electroanal. Chem.*, 2019, **832**, 399–407.

17 F. Ma, F. Liu, Y. Hou, H. Niu and C. Wang, *Synth. Met.*, 2020, **259**, 116235.
18 Y. Zhang, F. Liu, Y. Hou and H. Niu, *Synth. Met.*, 2019, **247**, 81–89.
19 D. Dai, M. Ouyang, L. Zhang, H. Fu, B. Tao, W. Li, X. Lv, R. Bai, Y. Dong and C. Zhang, *J. Mater. Chem. C*, 2022, **10**, 1339–1348.
20 D. Chlebosz, W. Goldeman, K. Janus, M. Szuster and A. Kiersnowski, *Molecules*, 2023, **28**, 2940.
21 M. Al Kobaisi, S. V. Bhosale, K. Latham, A. M. Raynor and S. V. Bhosale, *Chem. Rev.*, 2016, **116**, 11685–11796.
22 A. Das and S. Ghosh, *Macromolecules*, 2013, **46**, 3939–3949.
23 L. Gonzalez, C. Liu, B. Dietrich, H. Su, S. Sproules, H. Cui, D. Honecker, D. J. Adams and E. R. Draper, *Commun. Chem.*, 2018, **1**, 77.
24 Ş. Erten, Y. Posokhov, S. Alp and S. İçli, *Dyes Pigm.*, 2005, **64**, 171–178.
25 S. Guha, F. S. Goodson, S. Roy, L. J. Corson, C. A. Gravenmier and S. Saha, *J. Am. Chem. Soc.*, 2011, **133**, 15256–15259.
26 S. Halder, S. Roy and C. Chakraborty, *Sol. Energy Mater. Sol. Cells*, 2022, **234**, 111429.
27 R. I. Randle, L. Cavalcanti, S. Sproules and E. R. Draper, *Mater. Adv.*, 2022, **3**, 3326–3331.
28 R. I. Randle, A. M. Fuentes-Caparrós, L. P. Cavalcanti, R. Schweins, D. J. Adams and E. R. Draper, *J. Phys. Chem. C*, 2022, **126**, 13427–13432.
29 J. Y. Zheng, Q. Sun, J. Cui, X. Yu, S. Li, L. Zhang, S. Jiang, W. Ma and R. Ma, *Nanoscale*, 2023, **15**, 63–79.
30 H. Gong, A. Li, G. Fu, M. Zhang, Z. Zheng, Q. Zhang, K. Zhou, J. Liu and H. Wang, *J. Mater. Chem. A*, 2023, **11**, 8939–8949.
31 G. Nuroldayeva and M. P. Balanay, *Polymers*, 2023, **15**, 2924.
32 J. Chen, A. W. M. Tan, A. L.-S. Eh and P. S. Lee, *Adv. Energy Sustainability Res.*, 2022, **3**, 2100172.
33 V. Adams, J. Cameron, M. Wallace and E. R. Draper, *Chem. – Eur. J.*, 2020, **26**, 9879–9882.
34 Y. Luo, K. R. Kirker and G. D. Prestwich, *J. Control. Release*, 2000, **69**, 169–184.
35 A. Sionkowska, M. Gadomska, K. Musiał and J. Piątek, *Molecules*, 2020, **25**, 4035.
36 A. Sionkowska, M. Michalska-Sionkowska and M. Walczak, *Int. J. Biol. Macromol.*, 2020, **149**, 290–295.
37 C. J. Moore, *Environ. Res.*, 2008, **108**, 131–139.
38 A. K. Surca, G. Dražić and M. Mihelčič, *J. Sol-Gel. Sci. Technol.*, 2020, **95**, 587–598.
39 M. H. Penner, in *Food Analysis*, ed. S. S. Nielsen, Springer International Publishing, Cham, 2017, pp. 89–106.
40 Q. Huang, J. Hu, M. Yin, Y. Zhu and R.-T. Wen, *Sol. Energy Mater. Sol. Cells*, 2024, **267**, 112706.
41 L. Zheng, S. Zhang, Q. Yao, K. Lin, A. Rao, C. Niu, M. Yang, L. Wang and Y. Lv, *Ceram. Int.*, 2023, **49**, 13355–13362.
42 B. Hapke, in *Encyclopedia of Spectroscopy and Spectrometry*, eds. J. C. Lindon, G. E. Tranter and D. W. Koppenaal, Academic Press, Oxford, 3rd edn, 2017, pp. 931–935.
43 C. Yan, M. Cowie, C. Howcutt, K. M. P. Wheelhouse, N. S. Hodnett, M. Kollie, M. Gildea, M. H. Goodfellow and M. Reid, *Chem. Sci.*, 2023, **14**, 5323–5331.
44 H. Barrington, A. Dickinson, J. McGuire, C. Yan and M. Reid, *Org. Process Res. Dev.*, 2022, **26**, 3073–3088.
45 N. Bugeja, C. Oliver, N. McGrath, J. McGuire, C. Yan, F. Carlysle-Davies and M. Reid, *Digital Discovery*, 2023, **2**, 1143–1151.
46 C. Yan, C. Fyfe, L. Minty, H. Barrington, C. Jamieson and M. Reid, *Chem. Sci.*, 2023, **14**, 11872–11880.
47 L. F. Capitán-Vallvey, N. López-Ruiz, A. Martínez-Olmos, M. M. Erenas and A. J. Palma, *Anal. Chim. Acta*, 2015, **899**, 23–56.
48 E. R. Draper, J. J. Walsh, T. O. McDonald, M. A. Zwijnenburg, P. J. Cameron, A. J. Cowan and D. J. Adams, *J. Mater. Chem. C*, 2014, **2**, 5570–5575.
49 A. Zahra, R. Qureshi, M. Sajjad, F. Sadak, M. Nawaz, H. A. Khan and M. Uzair, *Expert Syst. Appl.*, 2024, **238**, 122172.
50 J. M. Baek, C. Yi and J. Y. Rhee, *Curr. Appl. Phys.*, 2018, **18**, 477–483.
51 J. G. Egan, G. Brodie, D. McDowall, A. J. Smith, C. J. C. Edwards-Gayle and E. R. Draper, *Mater. Adv.*, 2021, **2**, 5248–5253.
52 S. Nad, R. Jana, A. Datta and S. Malik, *J. Electroanal. Chem.*, 2022, **918**, 116484.
53 C. Gu, S. Wang, J. He, Y.-M. Zhang and S. X.-A. Zhang, *Chem.*, 2023, **9**, 1–14.

